Journal of the Ceramic Society of Japan 129 [6] 332-336 2021
DOI http://doi.org/10.2109/jcersj2.21009

JCS-Japan

NOTE

Synthesis, microstructure and electrochemical characterization of $NiMn_2O_4$ nanoparticles via a simple citric acid method

Hikaru ISHITSUKA[1], Yuya NAKAMURA[1], Hiroya ABE[2] and Yoshikazu SUZUKI[1,3,†]

[1] Graduate School of Pure and Applied Sciences, University of Tsukuba, Ibaraki 305–8573, Japan
[2] Joining and Welding Research Institute, Osaka University, 11–1 Mihogaoka, Ibaraki, Osaka 567–0047, Japan
[3] Faculty of Pure and Applied Sciences, University of Tsukuba, Ibaraki 305–8573, Japan

$NiMn_2O_4$ has an inverse spinel structure similarly to Co_3O_4 and $NiCo_2O_4$, but $NiMn_2O_4$ is much cheaper than these cobalt containing materials. Here, we report synthesis, microstructure and electrochemical characterization of $NiMn_2O_4$ nanoparticles via a simple citric acid method. $Ni(CH_3COO)_2{\cdot}4H_2O$ (1.5 mmol) and $Mn(CH_3COO)_2{\cdot}4H_2O$ (3.0 mmol) were dissolved in distilled water (25 mL), and citric acid (3.75 mmol) was added and stirred for 2 h to obtain transparent blue-green solution. The solution was open-heated at 90 °C for 24 h, and heated at 170 °C for 2 h to obtain a xerogel. The xerogel precursor was pestled and calcined at 400 °C for 4 h in air to obtain a $NiMn_2O_4$ powder. X-ray diffraction, N_2 adsorption/desorption and transmission electron microscopy with energy dispersive X-ray spectroscopy revealed that single-phase $NiMn_2O_4$ mesoporous nanoparticles were successfully synthesized from eco-friendly acetates ingredients by the low-cost citric acid method. The specific surface area and pore size of the $NiMn_2O_4$ mesoporous nanoparticles were 211.3 m^2/g and ~4 nm, respectively. The $NiMn_2O_4$ electrode successfully worked as a supercapacitor.

Key-words : $NiMn_2O_4$, Spinel, Electrochemical capacitor, Supercapacitor, Pseudocapacitor, Citric acid method

[Received January 9, 2021; Accepted March 24, 2021]

High-performance energy storage is crucial to realize our sustainable society, and electrochemical capacitors (or 'supercapacitors') are promising due to their fascinating characteristics, such as large power density, high-speed charging, long durability and relatively low cost.[1)–4)] A redox capacitor is a sort of supercapacitor that stores electrical energy as chemical energy via a reversible redox reaction near the interface between an electrode active material and an electrolyte solution. The redox capacitor is considered to store electric charge by stepwise changing the valence of the electrode active material. Despite having a redox capacity, its discharge-charging behavior is similar to that of an electric double layer capacitor (EDLC). Therefore, the redox capacitor is also called a 'pseudocapacitor'. A redox capacitor generally has a high specific capacity because all the electrode surfaces in contact with the electrolyte serve as ion adsorption/desorption points. Among them, hydrous RuO_2 systems have particularly high capacity, and it has been reported that the redox capacitor with $RuO_2{\cdot}nH_2O$ nanotube array electrode achieved even ~1300 F/g.[5)] However, since RuO_2-based redox capacitor is much more expensive than a conventional carbon-based EDLC, alternative electrode active materials for redox capacitors have been eagerly investigated. For example, Co-containing spinel-type oxides, such as Co_3O_4[6)–9)] and $NiCo_2O_4$,[10)–12)] are promising alternatives to RuO_2, but cobalt is still an expensive rare metal element.

To realize the further cost reduction of the electrode active materials, $NiMn_2O_4$ has attracted much attraction due to its low cost and non-toxicity. $NiMn_2O_4$ has an inverse spinel structure,[13),14)] similarly to $NiCo_2O_4$, but $NiMn_2O_4$ is much cheaper than Co_3O_4 and $NiCo_2O_4$. Hence, many research groups have synthesized various types of $NiMn_2O_4$ nanostructures via wet chemical processes, and applied them as redox capacitors.[15)–30)] Despite the promising results on high specific capacitance, many of these works used toxic or less environmentally-friendly ingredients, such as oxalate,[15),30)] nitrates[16)–21),23),27)–29)] and chlorides.[18),22),26)] Meanwhile, some of them used eco-friendly precursors, e.g., acetates.[24),25)] In these studies with acetates ingredients, however, somewhat costly organic additives were utilized, such as polyvinylpyrrolidone,[24)] polyvinylidene fluoride[25)] and N-methyl-2-pyrrolidone.[25)]

We think that $NiMn_2O_4$ nanoparticles can be synthesized from eco-friendly acetates ingredients with eco-friendly and low-cost citric acid. Here, we report eco-synthesis, microstructure and electrochemical characterization of $NiMn_2O_4$ nanoparticles via a simple citric acid method.

† Corresponding author: Y. Suzuki; E-mail: suzuki@ims.tsukuba.ac.jp

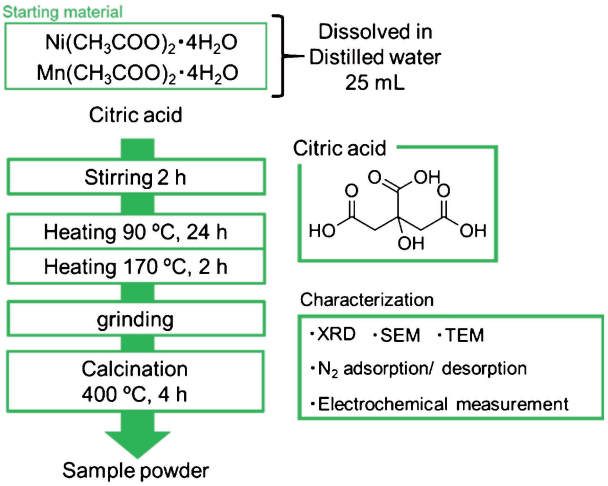

Fig. 1. Sample preparation procedure.

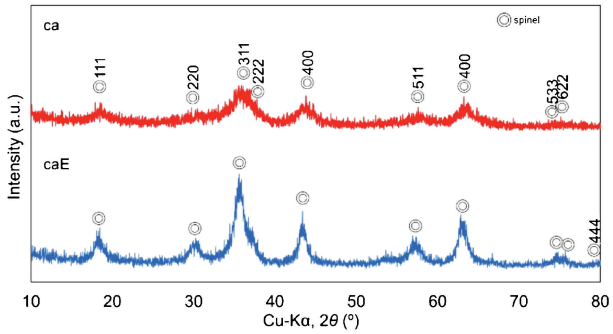

Fig. 2. XRD patterns of the $NiMn_2O_4$ powders. ca: citric acid added sample, and caE: citric acid and ethylene glycol co-added sample.

Figure 1 shows the sample preparation procedure. Commercially available nickel(II) acetate tetrahydrate ($Ni(CH_3COO)_2{\cdot}4H_2O$, >98 %, Fujifilm Wako, Japan), manganese(II) acetate tetrahydrate ($Mn(CH_3COO)_2{\cdot}4H_2O$, >99 %, Fujifilm Wako), and citric acid ($HOOCCH_2C(OH)(COOH)CH_2COOH$, gelation/chelating agent, >98 %, Fujifilm Wako) were used without additional purification. Typically, 1.5 mmol of $Ni(CH_3COO)_2{\cdot}4H_2O$, 3.0 mmol of $Mn(CH_3COO)_2{\cdot}4H_2O$ and 3.75 mmol of citric acid were carefully weighed. First, $Ni(CH_3COO)_2{\cdot}4H_2O$ and $Mn(CH_3COO)_2{\cdot}4H_2O$ powders were dissolved in 25 mL of distilled water by magnetic stirring for ~10 min. Then, citric acid powder was added and further stirred for 2 h to obtain transparent blue-green solution. The solution was open-heated (without sealing) in an oven at 90 °C for 24 h, and then successively heated at 170 °C for 2 h to obtain a xerogel. The xerogel precursor was pestled with agate mortar for 10 min, and then the precursor powder was calcined at 400 °C for 4 h in air to obtain a $NiMn_2O_4$ powder. The sample was named as 'ca' (= citric acid added sample).

Just as a comparison, another sample with a small amount of ethylene glycol was also tested, because ethylene glycol (ethane-1,2-diol) and other diols (e.g., butane-1,4-diol) also act as chelating agents (so called glycothermal method[31]) and ethylene glycol has been recently used to synthesize nickel manganate nanoparticles.[32] When adding the citric acid powder for the above 'ca' sample, 0.62 mL of ethylene glycol ($HOCH_2CH_2OH$, >99 %, Fujifilm Wako) was co-added. The sample was named as 'caE' (= citric acid and ethylene glycol co-added sample).

Phase analysis of the sample powders was conducted by X-ray diffraction (XRD, Multiflex, Cu-Kα, 40 kV and 40 mA, Rigaku). Microstructure was observed by scanning electron microscopy with energy-dispersive X-ray spectroscopy (SEM-EDS, SU-70, Hitachi/INCA System, Oxford) at the acceleration voltage of 15 kV and by transmission electron microscopy with EDS (TEM-EDS, JEM-2100F, JEOL). Scanning TEM (STEM) mode was also used. Specific surface areas and pore-size distributions of the sample powders were measured by nitrogen adsorption/desorption (SA-3100, Beckman Coulter) and analyzed by Brunauer–Emmett–Teller (BET) and Barrett–Joyner–Halenda (BJH) methods.

For the supercapacitor properties measurement, a $NiMn_2O_4$ working electrode was prepared with the 'ca' sample powder on a Ni foam (1 cm × 1 cm). The Ni foam was immersed in a 3 M HCl solution and cleaned by an ultrasonication for 20 min to remove the impurity layer. It was carefully washed with distilled water, ethanol and acetone. Then, the 'ca' sample paste with some ethanol was loaded on the cleaned Ni foam, and was annealed at 200 °C for 2 h in air. The obtained electrode was carefully washed with ethanol. A three-electrode method was used for the evaluation with an electrochemical analyzer (660A-G, ALS); saturated calomel electrode (SCE) was used as a reference electrode, Pt plate was used as a counter electrode, and a 1 M KOH aqueous solution was used as an electrolyte. The sample mass on the Ni foam was measured by electronic balance. The working electrode was evaluated by cyclic voltammetry (CV) and galvanostatic charge–discharge (GCD) test, similarly to our recent report on urchin-like $NiCo_2O_4$ particles.[12]

Figure 2 shows XRD patterns of the $NiMn_2O_4$ sample powders. Both 'ca' and 'caE' samples consisted of spinel phase. But only from these XRD patterns, it is difficult to specify the real chemical compositions of these powders (viz., $NiMn_2O_4$, $MnNi_2O_4$, $NiMn_2O_4$–$MnNi_2O_4$ solid solution or $NiMn_2O_4$/$MnNi_2O_4$ mixture). Preliminary elemental analyses suggested that the 'ca' sample was composed of almost pure $NiMn_2O_4$ (slightly Ni-rich than the stoichiometry), but the 'caE' sample was composed of 'near stoichiometric $NiMn_2O_4$/Mn-poor $NiMn_2O_4$ mixture', and hence the further evaluations were mainly focused on the 'ca' sample. Detail of the sample analysis is given in the Supporting Information.

Figure 3 shows N_2 adsorption/desorption isotherms and BJH pore-size distributions. Both 'ca' and 'caE' samples displayed IUPAC type-IV isotherms, which indicate that they were mesoporous materials. The specific surface areas for 'ca' and 'caE' were 211.3 and 99.1 m^2/g, respectively, which were in good agreement with broad and

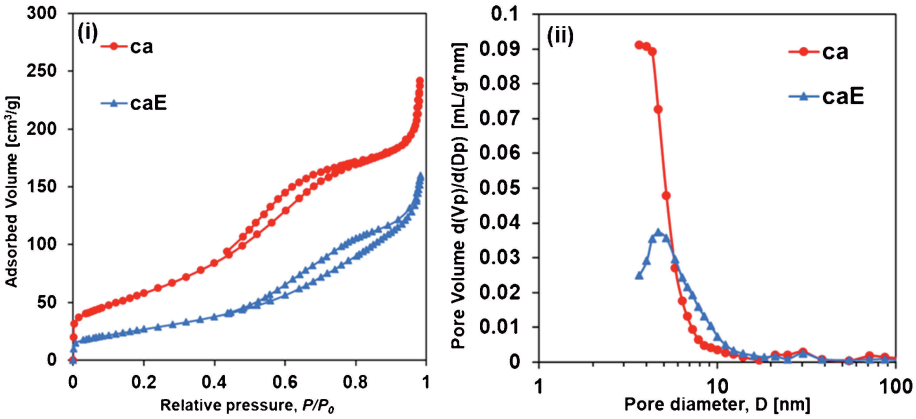

Fig. 3. N_2 adsorption/desorption measurements of the $NiMn_2O_4$ powders. (i) isotherms and (ii) BJH pore-size-distribution.

less-broad XRD patterns in Fig. 2. The BJH pore-size distribution curves clearly show the existence of mesopores. The typical pore sizes for these samples are estimated to be ~4 nm for 'ca' and ~5–10 nm for 'caE'. The formation of mesopores in the sample powders is attributable to the emission of H_2O and CO_2 gases during the thermal decomposition of precursors. However, these pores are too small for the penetration of electrolyte solution in an actual supercapacitor device. Further study on pore-structure control must be needed.

Since the 'ca' sample had larger BET surface area and sharper BJH pore-size distribution, it was further analyzed by SEM, TEM and STEM-EDS analyses. **Figure 4** shows SEM and low and high-resolution TEM images of the $NiMn_2O_4$ powder ('ca' sample). $NiMn_2O_4$ nanoparticles (typically ~50 nm) formed strongly aggregated secondary particles (SEM), and mesopores (~4 nm) were observed (TEM), which was in good agreement with the XRD and BJH analyses. **Figure 5** shows STEM-EDS elemental mapping images of the $NiMn_2O_4$ powder ('ca' sample). Ni, Mn and O atoms were homogeneously distributed in the sample. From the XRD, BJH and STEM-EDS analyses, it is concluded that a single-phase $NiMn_2O_4$ nanopowder with mesopores was successfully synthesized by a simple citric acid method.

Then the supercapacitor properties of the $NiMn_2O_4$ electrode were evaluated. **Figure 6** shows CV curves of the $NiMn_2O_4$ electrode with different scan rates at 5, 10, 20, 30, 40, 50, 75 and 100 mV s^{-1}.

Figure 7 shows GCD curves of the $NiMn_2O_4$ electrodes in the potential from 0 to 0.40 V at the different current densities. The specific capacitance can be calculated by the following formula,[33)]

$$C = \frac{I \times \Delta t}{m \times \Delta V}$$

where C (F/g) represents the specific capacitance of the working electrode, I (A) refers to the charge/discharge current, Δt (s) is the discharge time, m (g) is the mass of active material and ΔV (V) is potential drop during discharge. The specific capacitances of the $NiMn_2O_4$ electrodes in this

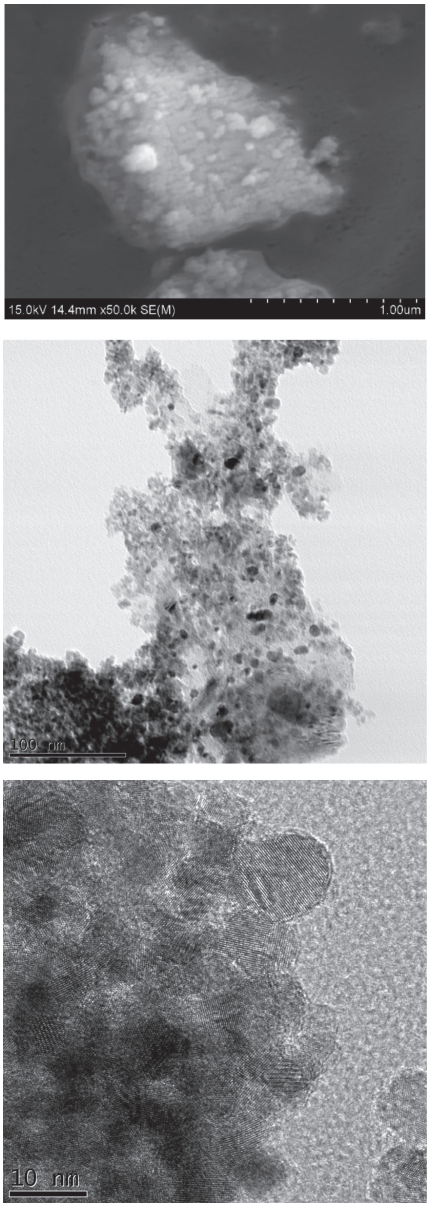

Fig. 4. SEM image and low and high-resolution TEM images of the $NiMn_2O_4$ powder ('ca' sample).

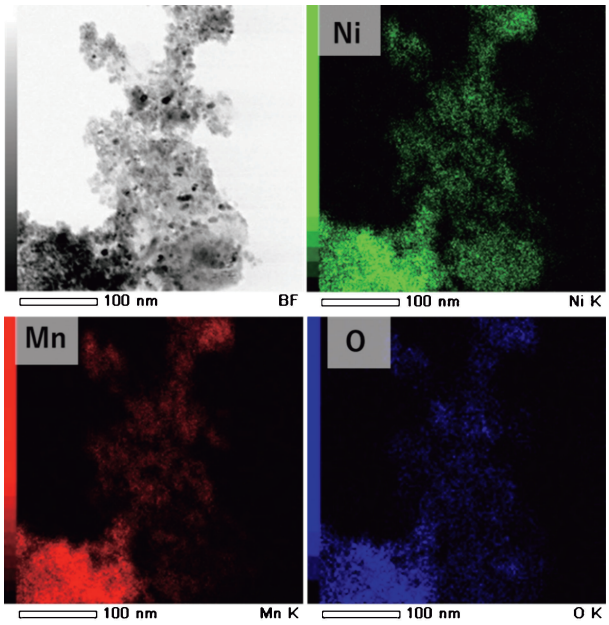

Fig. 5. STEM-EDS elemental mapping images of the $NiMn_2O_4$ powder ('ca' sample).

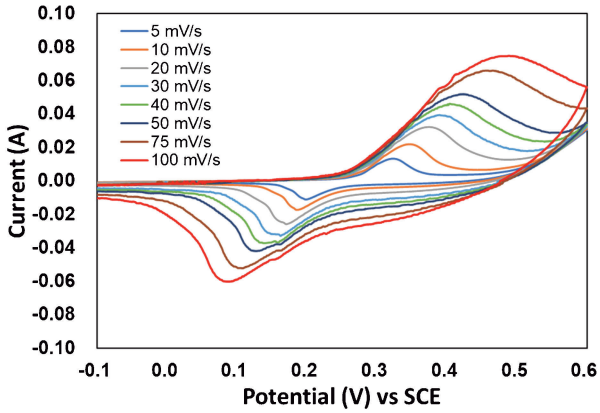

Fig. 6. CV curves with different scan rates of the $NiMn_2O_4$ electrodes. The $NiMn_2O_4$ sample mass on the Ni foam was ~10.1 mg/cm^2-Ni foam.

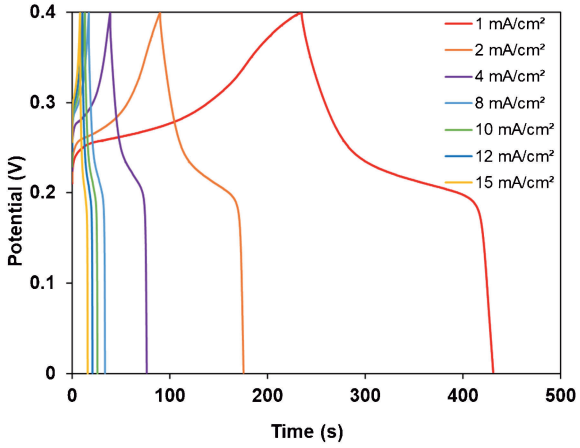

Fig. 7. GCD curves with the different current densities of the $NiMn_2O_4$ electrodes.

study were 48.6, 42.4, 37.0, 32.8, 31.4, 30.2, 28.7 F/g at the current density of 1, 2, 4, 8, 10, 12, 15 mA/cm^2, respectively.

The curve shapes of the CV curves (Fig. 6) and GCD curves (Fig. 7) of the $NiMn_2O_4$ electrode in this study were similar to those of the $NiCo_2O_4$ electrode in our previous study (U-10 sample with moderate performance).[12] In the previous study, urchin-like $NiCo_2O_4$ microstructure (in particular for the U-15 sample) is favorable for the penetration of liquid electrolyte, but in this study, such microstructure has not yet been realized. Actually, the current (Fig. 6) and the specific capacitance (from Fig. 7) of the $NiMn_2O_4$ electrode with equiaxed mesoporous (but microscopically aggregated) structure in this study were one-order smaller than those of the $NiCo_2O_4$ electrode with urchin-secondary particles.[12] Although $NiMn_2O_4$ has a potential for a replacement of expensive $NiCo_2O_4$, further tuning of the $NiMn_2O_4$ particle structure as well as the optimization of electrode structure will be required.

In conclusions, single-phase $NiMn_2O_4$ mesoporous nanoparticles were successfully synthesized from eco-friendly acetates ingredients by a low-cost citric acid method. The specific surface area and pore size of the $NiMn_2O_4$ mesoporous nanoparticles prepared with citric acid were 211.3 m^2/g and ~4 nm, respectively. The $NiMn_2O_4$ electrode in this study successfully worked as a supercapacitor, but the further tuning of the particle shape (e.g., urchin-like structure) is needed to further improve the electrochemical performance.

Acknowledgment This work was supported by JSPS KAKENHI Grant Number JP16H04212 and JP20H02431 for Basic Research: Category B, and Joint Research Project of JWRI, Osaka University. We thank the Open Facility Network Office, Research Facility Center for Science and Technology, University of Tsukuba, for the electrochemical measurements. We also thank anonymous reviewers for their valuable comments to improve the manuscript.

References

1) P. Simon and Y. Gogotsi, *Nat. Mater.*, 7, 845–854 (2008).
2) G. P. Wang, L. Zhang and J. J. Zhang, *Chem. Soc. Rev.*, 41, 797–828 (2012).
3) C. Zhong, Y. D. Deng, W. B. Hu, J. L. Qiao, L. Zhang and J. J. Zhang, *Chem. Soc. Rev.*, 44, 7484–7539 (2015).
4) A. Gonzalez, E. Goikolea, J. A. Barrena and R. Mysyk, *Renew. Sust. Energ. Rev.*, 58, 1189–1206 (2016).
5) C. C. Hu, K. H. Chang, M. C. Lin and Y. T. Wu, *Nano Lett.*, 6, 2690–2695 (2006).
6) S. K. Meher and G. R. Rao, *J. Phys. Chem. C*, 115, 15646–15654 (2011).
7) X. H. Xia, J. P. Tu, Y. J. Mai, X. L. Wang, C. D. Gu and X. B. Zhao, *J. Mater. Chem.*, 21, 9319–9325 (2011).
8) S. L. Xiong, C. Z. Yuan, M. F. Zhang, B. J. Xi and Y. T. Qian, *Chem.-Eur. J.*, 15, 5320–5326 (2009).
9) K. Fukui and Y. Suzuki, *Ceram. Int.*, 45, 9288–9292 (2019).
10) T. Y. Wei, C. H. Chen, H. C. Chien, S. Y. Lu and C. C.

Hu, *Adv. Mater.*, 22, 347–351 (2010).
11) Y. Lei, J. Li, Y. Y. Wang, L. Gu, Y. F. Chang, H. Y. Yuan and D. Xiao, *ACS Appl. Mater. Inter.*, 6, 1773–1780 (2014).
12) K. Fukui, Y. Nakamura, H. Abe and Y. Suzuki, *J. Ceram. Soc. Jpn.*, 127, 843–848 (2019).
13) A. Sagua, G. M. Lescano, J. A. Alonso, R. Martinez-Coronado, M. T. Fernandez-Diaz and E. Moran, *Mater. Res. Bull.*, 47, 1335–1338 (2012).
14) G. Ashcroft, I. Terry and R. Gover, *J. Eur. Ceram. Soc.*, 26, 901–908 (2006).
15) H. Pang, J. W. Deng, S. M. Wang, S. J. Li, J. M. Du, J. Chena and J. S. Zhang, *RSC Adv.*, 2, 5930–5934 (2012).
16) M. Zhang, S. H. Guo, L. Zheng, G. N. Zhang, Z. P. Hao, L. P. Kang and Z. H. Liu, *Electrochim. Acta*, 87, 546–553 (2013).
17) K. V. Sankar, S. Surendran, K. Pandi, A. M. Allin, V. D. Nithya, Y. S. Lee and R. K. Selvan, *RSC Adv.*, 5, 27649–27656 (2015).
18) H. L. Yan, T. Li, K. W. Qiu, Y. Lu, J. B. Cheng, Y. X. Liu, J. Y. Xu and Y. S. Luo, *J. Solid State Electr.*, 19, 3169–3175 (2015).
19) H. M. Wei, J. X. Wang, L. Yu, Y. Y. Zhang, D. W. Hou and T. F. Li, *Ceram. Int.*, 42, 14963–14969 (2016).
20) G. Liu, J. Shao, Y. J. Gao, Z. Chen and Q. T. Qu, *Chinese J. Chem.*, 35, 67–72 (2017).
21) M. Y. Arsent'ev, N. Y. Koval'ko, A. V. Shmigel', P. A. Tikhonov and M. V. Kalinina, *Glass Phys. Chem.*, 43, 376–379 (2017).
22) U. J. Chavan and A. A. Yadav, *J. Mater. Sci.-Mater. El.*, 28, 4958–4964 (2017).
23) J. Bhagwan, S. Rani, V. Sivasankaran, K. L. Yadav and Y. Sharma, *Appl. Surf. Sci.*, 426, 913–923 (2017).
24) A. Ray, A. Roy, M. Ghosh, J. A. Ramos-Ramon, S. Saha, U. Pal, S. K. Bhattacharya and S. Das, *Appl. Surf. Sci.*, 463, 513–525 (2019).
25) S. K. Hussain, G. Nagaraju, S. C. Sekhar and J. S. Yu, *J. Power Sources*, 439, 227088 (2019).
26) P. Ahuja, S. K. Ujjain, R. K. Sharma and G. Singh, *RSC Adv.*, 4, 57192–57199 (2014).
27) Y. Ouyang, Y. Y. Feng, H. J. Zhang, L. Liu and Y. Wang, *ACS Sustain. Chem. Eng.*, 5, 196–205 (2017).
28) M. R. Kim, R. M. NaiduKalla, S. Kim, M. R. Kim and I. Kim, *ChemElectroChem*, 4, 1214–1221 (2017).
29) H. H. Nan, W. Q. Ma, Z. X. Gu, B. Y. Geng and X. J. Zhang, *RSC Adv.*, 5, 24607–24614 (2015).
30) S. Sahoo, S. J. Zhang and J. J. Shim, *Electrochim. Acta*, 216, 386–396 (2016).
31) M. Inoue, H. Otsu, H. Kominami and T. Inui, *Nippon Kagaku Kaishi*, 1991, 1358–1360 (1991) [in Japanese].
32) A. Ray, A. Roy, S. Saha, M. Glosh, S. R. Chowdhury, T. Maiyalagan, S. K. Bhattacharya and S. Das, *Langmuir*, 35, 8257–8267 (2019).
33) L. Feng, Y. Zhu, H. Ding and C. Ni, *J. Power Sources*, 267, 430–444 (2014).